International Journal of Nanoelectronics and Materials
IJNeaM
ISSN 1985-5761 | E-ISSN 2232-1535

Numerical prediction of effective elastic properties of single-wall carbon nanotubes-poly(methyl methacrylate) nanocomposites for orthopedic surgeries application

Ibrahim Haddouch [a] *, Mabrouk Benhamou [b], Ilias Mouallif [a], Oumaima Zhouri [a], and Elyazid Ismaili [a]

[a]*L2MC, ENSAM, Moulay Ismail University, P.O. Box 15290, Al Mansour, Meknès, Morocco*
[b]*Dynamics of Complex Sytems Laboratory, Faculty of Sciences, Moulay Ismail University P.O. Box 11201, Meknès, Morocco*
∗Corresponding author. e-mail: ibrahim.haddouch@edu.umi.ac.ma

Received 21 September 2024, Revised 09 October 2024, Accepted 28 November 2024

ABSTRACT

This study undertakes a numerical examination of the effective elastic characteristics of various nanocomposites comprising poly(methyl methacrylate) (PMMA) as the matrix, reinforced with armchair or zigzag single-walled carbon nanotubes. Such composites serve as biomaterial implants in the field of medicine. Employing COMSOL Multiphysics® Software, specifically the Solid Mechanics Physics module within the Structural Mechanics module, we conducted analyses on three-dimensional representative volume elements for static evaluations. Our focus was on determining the effective elastic properties, encompassing elastic moduli in X, Y, and Z directions, as well as shear moduli in XY, YZ, and ZX planes. The investigation encompassed varying volume fractions of the reinforcement material, spanning low and medium concentrations. Additionally, the elastic modulus in the x-direction underwent validation using the Rule of Mixture, providing a thorough assessment of the polymer/nanotube composite's elastic modulus in the X-direction and confirming the accuracy of this specific outcome. Ultimately, our work contributes to the advancement of materials and technologies by furnishing significant insights into the effective elastic properties of the examined nanocomposites, across various levels of carbon nanotube reinforcement, while ensuring the reliability of the obtained elastic modulus in the x-direction through validation using the Rule of Mixture.

Keywords: *Carbon nanotubes, Nanocomposite, PMMA, Orthopedic surgeries application, Effectives elastic properties, Homogenization method*

1. INTRODUCTION

Nanocomposites are multiphase solid materials with at least one phase dimension of less than 100 nanometers [1]. Such materials are usually the combination of a massive matrix with a nanoscale reinforcement phase of different properties resulting from the structural and chemical differences. The nanoscale reinforcement is dispersed within the matrix during the development of the composite. The mass content of the nanoparticles introduced is often very low (between 0.5% and 5%) because of the low percolation threshold. This is typically the case for non-spherical nanoparticles with a high form factor (clays in the form of sheets or carbon nanotubes in the form of fibers, for instance). Depending on the constituent of the matrix, there are several types of nanocomposites: polymer matrix nanocomposites, ceramic matrix nanocomposites or metal matrix nanocomposites.

In this work, we were interested in a mechanical study of nanocomposites composed of a polymer matrix with dispersed carbon nanotubes [2].

The mechanical properties of nanocomposites are different from those of traditional composite materials because of the high surface-to-volume ratio of the reinforcement and its large form factor. The reinforcement can be in the form of particles (minerals), sheets (exfoliated clays) or fibers (carbon nanotubes). The matrix-reinforcement interface has a large surface area that is typically an order of magnitude larger than that of a traditional composite material. This interface implies that a small amount of nanoscale reinforcement can have an observable effect on the macroscopic properties of the composite. For example, the addition of carbon nanotubes improves the electrical and thermal conductivities and mechanical properties of composite material. Other types of nanoparticles can lead to improvements in optical, dielectric, fire resistance or mechanical properties of the nanocomposites.

Carbon nanotubes (CNTs), as reinforcement, play a major role the development of the mechanical properties of polymer nanocomposites [3]. Their low diameter and their high aspect ratio make them an ideal material to improve the properties of the polymer matrix, compared to glass, carbon or aramid fibers. More precisely, nanotubes “SWCNTS” should improve the elasticity modulus of the polymer matrix. It is noted that a CNT is a hundred times lighter and six times stronger than steel. To favor more the adhesion between polymer matrix and reinforcement, CNTs

are usually functionalized by grafting short organic chains on their surface. The typical characteristics of carbon nanotubes (CNTs) dispersed in a polymer matrix are as follows: their diameter is approximately 10 nm, their volume fraction is about 3%, their total number is on the order of 10^{15}, their specific surface area is around 100 m^2/g, and their aspect ratio is approximately 1000. Another important parameter of CNTs is their interparticle distance, which depends on the volume fraction. As noted in Ref. [4], the relative distance between CNTs increases as the volume fraction decreases. For instance, for single-walled carbon nanotubes (SWCNTs) with a diameter of 3.2 nm, a volume fraction of 3% was reported [4].

In the present work, we focus only on Armchair or Zigzag SWCNTs, each is characterized by two chiral indices (n, m) [5]. For the numerical study, we have chosen (5,5) Armchair and (9,0) Zigzag SWCNTs. The term "Armchair" denotes the specific arrangement of carbon atoms along the nanotube sidewalls. In an Armchair SWCNT, the rows of carbon atoms run parallel to the tube axis, resembling the arms of a chair, hence the name. The (5,5) Armchair SWCNT has a well-defined and symmetric structure due to the equal values of n and m [6, 7]. This symmetry can make it easier to use in a variety of applications, such as electronics [8] and nanotechnology [6, 9]. Understanding the properties and behavior of the specific SWCNTs structures, as (5,5) Armchair SWCNTs, is essential for harnessing their unique characteristics in advanced technologies and materials. The term "Zigzag" indicates the specific arrangement of carbon atoms along the sidewalls of the nanotube [9]. In a Zigzag SWCNT, the rows of carbon atoms run parallel to the tube axis, forming a distinctive Zigzag pattern. Zigzag SWCNTs have a relatively simple and symmetric structure compared with other chiralities, such as Armchair or chiral SWCNTs [9]. This simple structure can be advantageous in certain applications. The elastic properties of both SWCNTs used in this paper are extracted from [10].

For the study, the chosen matrix as host phase was poly(methyl methacrylate) (PMMA). The latter is a synthetic polymer which belongs to acrylic polymers family [11]. Such a polymer is a transparent thermoplastic with various applications. In addition, it is known for its exceptional optical clarity and transparency [12] and often used as a lightweight alternative to glass in applications where the optical properties are crucial [12], such as in the production of clear plastic sheets, lenses and displays. Despite its transparency, PMMA is remarkably impact-resistant, making it suitable for applications where safety and durability are essential [13]. It is also used in the production of safety glasses, protective shields and riot gear. PMMA exhibits excellent resistance to UV radiation [14] and weathering [15], making it suitable for outdoor applications. It is commonly used for outdoor signs [16].

PMMA bone cement is commonly used in the joint replacement surgeries, such as hip and knee replacements [17, 18]. It serves as an adhesive to fix the artificial joint components (prostheses) to the existing bone [18, 19]. PMMA cement forms a strong bond with the bone and the implant, providing stability and allowing patients to regain mobility and reduce pain [18]. PMMA can be used to create orthopedic spacers in cases of bone infection or in the revision joint replacement surgeries [18]. These spacers are typically temporary and help to maintain the joint space while treating or managing infection [18]. In some cases, PMMA can be used to create custom orthopedic implants [20], particularly for patients with complex or irregular bone shapes [18, 21]. These implants are typically temporary and can provide a stable foundation for bone healing [20]. PMMA can be used to secure the fixation pins or screws in the orthopedic surgeries, helping to stabilize the fractures or maintain the position of the implants. Orthopedic surgeons and medical professionals carefully evaluate the choice of materials, surgical techniques, and patient-specific factors to ensure the best possible outcomes in orthopedic procedures involving PMMA [20]. Advances in materials and techniques continue to improve the safety and effectiveness of PMMA-based orthopedic applications [9, 18, 20, 21]. The elastic properties of PMMA are described in [22].

The mean goal of the present work is a numerical study of effectives elastic properties “EEP” of some kinds of nanocomposites formed by PMMA (as matrix) reinforced with (5,5) Armchair or (9,0) Zigzag SWCNTs. The analysis was achieved using COMSOL Multiphysics® Software. Our study focused on the investigation of EEP, including the elastic moduli in X, Y, and Z directions, as well as shear moduli in XY, YZ, and ZX plans, versus the volume fraction of the reinforcement material (SWCNTs in our case). The elastic modulus in the x-direction was validated using the Mixture Rule. By considering this rule, the study provides a rigorous assessment of the elastic modulus in the x-direction of PMMA-SWCNT nanocomposites and verifies the accuracy of this specific result. Finally, we think that the present work may contribute to the development of advanced materials and technologies by providing valuable information on EEP of PMMA-SWCNT nanocomposites, with different levels of the carbon nanotubes reinforcement [23–26].

The remaining of presentation is organized as follows. First, we describe the considered materials and precise the used numerical methodology. Second, we present the results and discussion. Finally, some concluding remarks are present at the end of the manuscript.

2. MATERIALS AND METHODOLOGY

2.1. Materials

PMMA is a transparent thermoplastic known for its exceptional optical clarity and transparency. It is commonly used as a lightweight alternative to glass in applications where optical properties are crucial, such as clear plastic sheets, lenses, and displays. It is also impact-resistant, making it suitable for safety glasses, protective shields and riot gear. Such a polymer exhibits an excellent resistance to UV radiation and weathering, making it suitable for outdoor applications like outdoor signs. PMMA bone cement is

commonly used in joint replacement surgeries, providing stability and allowing patients to regain mobility. The elastic properties are regrouped in Table 1 [25].

The study involves the incorporation of SWCNTs into PMMA matrix, whose general structures are shown in Figure 1. Two types of SWCNTs are considered, namely (5,5) Armchair and (9,0) Zigzag single wall SWCNTs. These kinds of SWCNTs have unique properties and structures that make them suitable for various applications.

The elastic properties of both types of SWCNTs are given in Table 2 [12].

2.2. Representative Volume Element (RVE)

Representative volume element (RVE) takes the form of a cubic cross-section of PMMA matrix embedded by: (i) (5,5) Armchair or (ii) (9,0) Zigzag SWCNTs. These materials are tightly arranged to form an outer radius of 1.5 nm [24] and has a thickness of 0.34 nm. The size of RVE, and the length of SWCNT, L_{cnt}, are precisely defined based on the desired CNT volume fraction, v_{cnt}. The latter is given by the following relation [25].

$$v_{cnt} = \frac{V_{CNT}}{V_{RVE}} = \frac{\pi(r_o^2 - r_i^2)L_{cnt}}{(a^2 - \pi r_i^2)L_{RVE}} \quad (1)$$

Here, V_{CNT} accounts for the volume of SWCNT, V_{RVE} for the volume of cubic RVE and r_o and r_i are the outer and inner radii. The size of RVE is as follows

$$a = \sqrt{\pi r_i^2 + \frac{\boldsymbol{\pi(r_o^2 - r_i^2)}}{\boldsymbol{v_{cnt}}}} \quad (2)$$

The analyses were carried out utilizing a three-dimensional Finite Element Model of RVE Figure 2. This model was developed using COMSOL Multiphysics®. All constituents were represented within this model using Cell Periodicity. Various perspectives of a typical FE mesh of RVE. The mesh selection was a free triangular in the side of end CNT and the mesh selected for the other side was swept as shown in Figure 2. The chosen mesh is characterized by a relatively low density, since the analyses conducted were linear and RVE geometry exhibited no geometric non-linearity. To determin the elastic properties, the Cell Periodicity was used. Such a technique involves applying a small normal displacement on one side while fully constraining the opposite side. Similarly, for the calculation of shear moduli, the three planes were subjected to shear loading by applying a shear displacement to one face and fully constraining the opposite face. To represent the homogenized engineering behavior of RVE, reflecting the material macroscopic properties, periodic boundary conditions were implemented within RVE. In fact, these conditions were applied using constraint equations on opposite faces, ensuring that the model accurately captures the overall behavior of the material.

Table 1. Elastic properties of PMMA

Young's modulus, E (GPa)	Shear modulus, G (GPa)	Poisson ratio, ν
2.4	1.7	0.37

Table 2. Orthotropic elastic properties of SWCNTs

Elastic quantities (GPa)	(5,5) Armchair CTN	(9,0) Zigzag CTN
E_l	1398	1411
E_θ	1484	1411
E_r	1300	1210
$\nu_{\theta l}$	0.175	0.225
$\nu_{\theta r}$	0.17	0.17
ν_{lr}	0.1675	0.215
$G_{\theta l}$	631	576
$G_{\theta r}$	634	430
G_{lr}	385	602

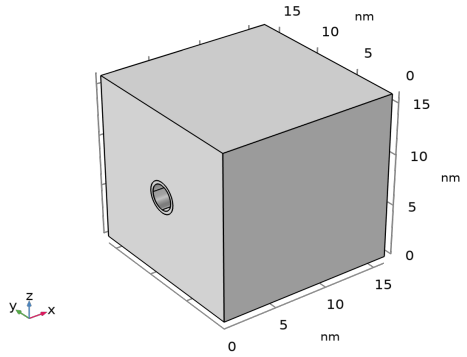

Figure 1. Geometry

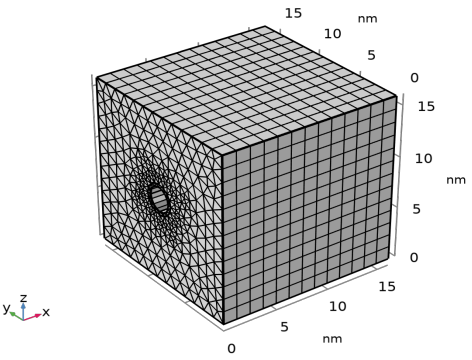

Figure 2. Model meshed

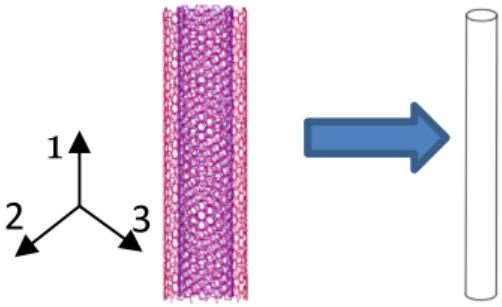

Figure 3. Equivalent geometric representation for modeling SWCNTs [26]

2.3. Periodic Boundary Condition on RVE

It is of utmost importance to carefully define appropriate boundary conditions for RVE when assessing the elastic moduli effectively. These boundary conditions should accurately replicate the real deformation occurring within the nanocomposite under specific loading conditions. In our current analysis, we employ the boundary conditions for RVE under different loading conditions as originally developed [27–29]. They skillfully established these conditions through the application of symmetry and periodicity principles. These boundary conditions are essential for predicting the mechanical properties of the conventional composite using RVE approach, and we utilize them in our finite element model. The subsequent sections will detail the specific displacement boundary conditions applied to the finite element model for scenarios involving normal loading, transverse shear loading and longitudinal shear loading. These conditions are crucial to compute the various elastic moduli accurately.

The following equations represent the boundary conditions for estimating the Young's moduli in the three directions, x, y and z:

- Boundary condition to compute E_{xx}:

$$u_{11}(0,y,z) = u_{22}(x,0,z) = u_{33}(x,y,0) = 0, u_{11}(a,y,z) = \delta_{xx} \quad (3)$$

- Boundary condition to compute E_{yy}:

$$u_{11}(0,y,z) = u_{22}(x,0,z) = u_{33}(x,y,0) = 0, u_{22}(x,a,z) = \delta_{yy} \quad (4)$$

- Boundary condition to compute E_{zz}:

$$u_{11}(0,y,z) = u_{22}(x,0,z) = u_{33}(x,y,0) = 0, u_{33}(x,y,a) = \delta_{zz} \quad (5)$$

In addition, the following equations represent the boundary conditions for estimating the shear moduli in three directions, X, Y and Z [23]:

- Boundary condition to compute G_{xy}:

$$u_{11}(x,0,z) = u_{22}(x,0,z) = u_{33}(x,0,z) = 0, u_{11}(x,a,z) = \delta_{l} \quad (6)$$

- Boundary condition to compute G_{xz}:

$$u_{11}(x,y,0) = u_{22}(x,y,0) = u_{33}(x,y,0) = 0, u_{22}(x,y,a) = \delta_{t} \quad (7)$$

- The same Boundary condition as precedent used to compute G_{yz}:

$$u_{11}(x,0,z) = u_{22}(x,0,z) = u_{33}(x,0,z)0, u_{11}(a,y,z) = \delta_{l} \quad (8)$$

In formulae above, quantities u_{11}, u_{22} and u_{33} represent the displacement components in X, Y and Z directions, respectively, δ_{xx} denotes the constant displacement value applied in X-direction on X = a plane of RVE, δ_{yy} represents the constant displacement value applied in Y-direction on the Y = a plane of RVE and δ_{zz} is the constant displacement value applied in Z-direction on Z = a plane of RVE. The shear loading, δ_l, is the constant displacement value applied in X-direction at Y = a face of RVE, the shear loading, δ_t, is the constant displacement value applied in Z-direction at Z = a face of RVE. All these equations are illustrated by Figure 4.

3. RESULTS AND DISCUSSION

3.1. Low Concentration

In this section, we explore the effects of using small amounts of SWCNTs as reinforcement on mechanical properties.

PMMA is considered as an isotropic material which exhibits the same mechanical properties in all directions. Its mechanical properties such as Young's modulus and shear modulus are generally the same in all directions and have as values 2.4E9 Pa and 1.7E9 Pa, respectively. This means that PMMA response to mechanical stress is independent of the orientation of the stress or strain. However, when we introduce a mere 1% concentration of (5,5) Armchair SWCNTs, we observe a substantial decrease of Young's modulus (Exx) of PMMA, which now stands at 1.7832E10 Pa. Upon further elevating the concentration to 10%, the axial Young's modulus undergoes a pronounced reduction reaching 1.43439E11 Pa. A parallel pattern emerges when considering PMMA reinforced with 1% of (9,0) Zigzag SWCNTs. In this case, the initial Young's modulus (Exx) measures 1.79619E10 Pa, but when the concentration increases to 10%, the axial Young's modulus diminishes to 1.45025E11Pa (see Tables 3, 4 and Figure 5).

Similar trends can be observed for Young's moduli in Y-direction. At 1% concentration of (5,5) Armchair SWCNTs, Young's modulus, Eyy, of the nanocomposite is

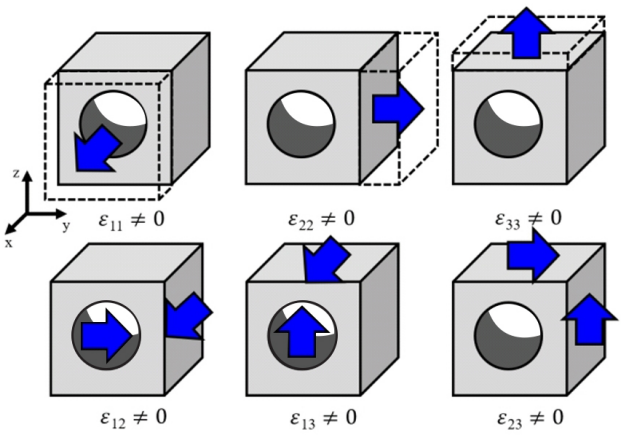

Figure 4. Boundary conditions necessary to calculate all elastic properties [24]

4.05955E9 Pa, but this such a value significantly ascends to 6.40204E9Pa at 10% of (5,5) Armchair SWCNT concentration. When we examine PMMA fortified with 1% of (9,0) Zigzag SWCNT, Young's modulus, Eyy, stands at 4.05827E9 Pa. With a subsequent increase in the concentration to 10%, Young's modulus experiences a decrease, measuring 6.36629E9 Pa (refer to Tables 3, 4 and Figure 6).

Concerning the Young's modulus in Z-direction, at 1% concentration of (5,5) Armchair SWCNTs, it amounts at the value 4.05925E9 Pa. However, at 10% concentration, the Z-direction Young's modulus markedly increases to 6.36629E9 Pa. This trend is also observed in the case of PMMA reinforced by 1% of (9,0) Zigzag SWCNTs, where Young's modulus (Ezz) starts at 4.0579E9 Pa and eventually reaches the value 6.36059E9Pa at a 10% concentration (refer to Tables 3, 4 and Figure 7).

Shear moduli for a nanocomposite exhibits notable variations at different concentrations of SWCNTs. Specifically, at 1% concentration of (5,5) Armchair SWCNTs, shear modulus (Gxy) of the nanocomposite measures 1.00193E9 Pa, reflecting a significant decrease. Upon increasing the concentration to 10%, the shear modulus drops further to 1.72986E10 Pa. Similarly, when incorporating 1% of (9,0) zigzag SWCNTs into PMMA matrix, the value of the shear modulus, Gxy is 1.00195E9 Pa. A subsequent increase in concentration to 10% leads to a shear modulus reduction measuring 1.72986E10 Pa (refer to Tables 5, 6) and (Figure 8).

The trend persists when analyzing the shear modulus, Gyz, the nanocomposite. At a 1% concentration of (5,5) Armchair SWCNTs, the value of this modulus is 9.83964E8 Pa. Elevating the concentration to 10% yields a shear modulus, Gyz, of 1.45758E9 Pa. For PMMA reinforced by 1% of (9,0) zigzag SWCNTs, the shear modulus, Gyz, is 9.82398E8 Pa at 1% concentration and increases to the value 1.43950E9Pa at 10% of (9,0) zigzag SWCNTs concentration (refer to Tables 5,6 and Figure 9). Examining the shear modulus, Gxz, for PMMA, at a 1% concentration of (5,5) Armchair SWCNTs, it measures 1.00164E9 Pa. With an increase to 10% concentration, this shear modulus reaches the value of 1.75344E9 Pa. For PMMA reinforced by 1% of (9,0) Zigzag SWCNTs, the shear modulus, Gxz, is 1.00197E9 Pa at a 1% concentration and rises to the value 1.75906E9 Pa at 10% (see Tables 5,6) and (Figure 10). Comparing the two types of SWCNTs at a 1% concentration, (9,0) zigzag SWCNTs reinforcement results in a slightly higher elastic properties compared to (5,5) Armchair SWCNTs reinforcement. However, when the concentration is increased to 9%, the two types of nanotubes lead to a significant increase of the elastic properties.

3.2. Medium Concentration

In this section, we analyze the effects of using medium amounts of SWCNTs as reinforcement on mechanical properties.

Tables, 7–10 and Figures 11–16 below depict the elastic properties of polymer-nanotube composites. The composite

Table 3. Young's Moduli of nanocomposite PMMA-(5,5) Armchair, Cell Periodicity

VF (%)	E_{xx} (Pa)	E_{yy} (Pa)	E_{zz} (Pa)
0.01	1.78320E10	4.05955E9	4.05925E9
0.02	3.11143E10	4.28464E9	4.37773E9
0.03	4.49340E10	4.51396E9	4.59741E9
0.04	5.87537E10	4.74923E9	4.82279E9
0.05	7.28453E10	5.00233E9	5.06526E9
0.06	8.72994E10	5.26053E9	5.30203E9
0.07	1.00802E11	5.52553E9	5.56647E9
0.08	1.14894E11	5.80751E9	5.83660E9
0.09	1.29348E11	6.08826E9	6.0841E9
0.10	1.43439E11	6.40204E9	6.36629E9

Table 4. Young's Moduli of nanocomposite PMMA-(9,0) Armchair, Cell Periodicity

VF (%)	E_{xx} (Pa)	E_{yy} (Pa)	E_{zz} (Pa)
0.01	1.79619E10	4.05827E9	4.0579E9
0.02	3.14314E10	4.35494E9	4.34925E9
0.03	4.58855E10	4.56893E9	4.57463E9
0.04	6.02943E10	4.78943E9	4.79432E9
0.05	7.44312E10	5.04248E9	5.03678E9
0.06	8.85228E10	5.29064E9	5.28495E9
0.07	1.02660E11	5.53799E9	5.53230E9
0.08	1.16479E11	5.80894E9	5.79755E9
0.09	1.30868E11	6.06832E9	6.06328E9
0.10	1.45025E11	6.36629E9	6.36059E9

Table 5. Shear Moduli of nanocomposite PMMA-(5,5) Armchair, Cell Periodicity

VF (%)	G_{xy} (Pa)	G_{xz} (Pa)	G_{yz} (Pa)
0.01	1.00193E9	1.00164E9	9.83964E8
0.02	2.63529E9	1.06715E9	9.91682E8
0.03	4.21205E9	1.14135E9	1.04874E9
0.04	5.86850E9	1.22305E9	1.10580E9
0.05	7.55911E9	1.30261E9	1.16546E9
0.06	9.25541E9	1.38243E9	1.22111E9
0.07	1.11851E10	1.47324E9	1.27958E9
0.08	1.31603E10	1.56619E9	1.33945E9
0.09	1.66583E9	1.66206E9	1.4068E9
0.10	1.72986E10	1.75344E9	1.45758E9

Table 6. Shear Moduli of nanocomposite PMMA-(9,0) Armchair, Cell Periodicity

VF (%)	G_{xy} (Pa)	G_{xz} (Pa)	G_{yz} (Pa)
0.01	1.00195E9	1.00197E9	9.82398E8
0.02	2.63529E9	1.07465E9	9.84651E8
0.03	4.21205E9	1.14885E9	1.04030E9
0.04	5.86850E9	1.22493E9	1.09736E9
0.05	7.55911E9	1.31011E9	1.15441E9
0.06	9.25541E9	1.38993E9	1.20725E9
0.07	1.11851E10	1.47887E9	1.26572E9
0.08	1.31603E10	1.57155E9	1.32418E9
0.09	1.66626E9	1.66654E9	1.39162E9
0.10	1.72986E10	1.75906E9	1.43950E9

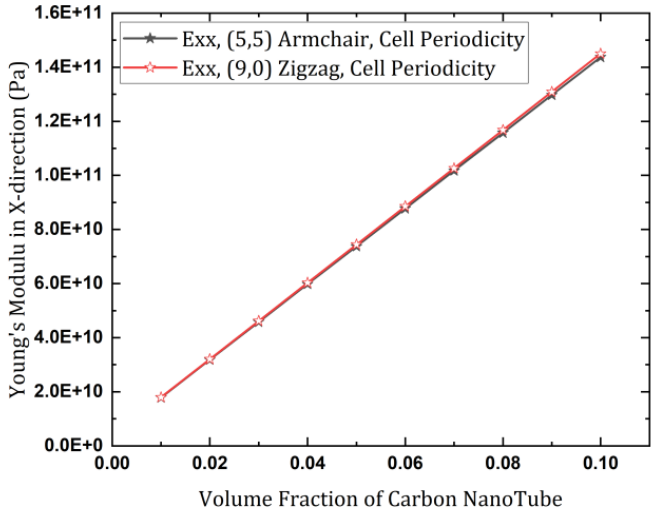

Figure 5. Young's moduli in X-direction

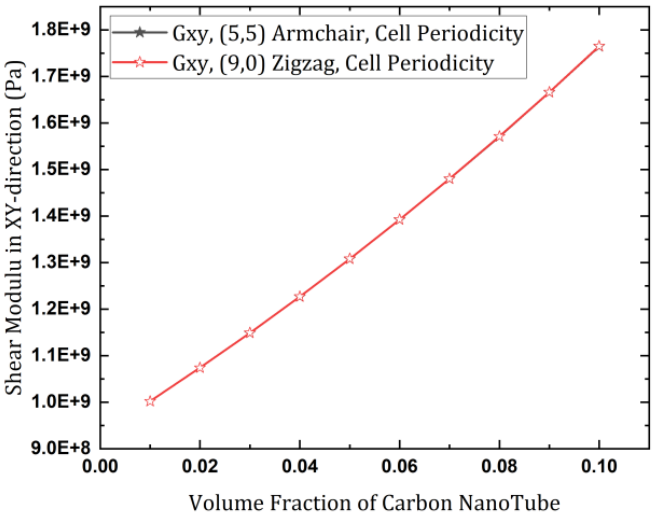

Figure 8. Shear moduli in XY-direction

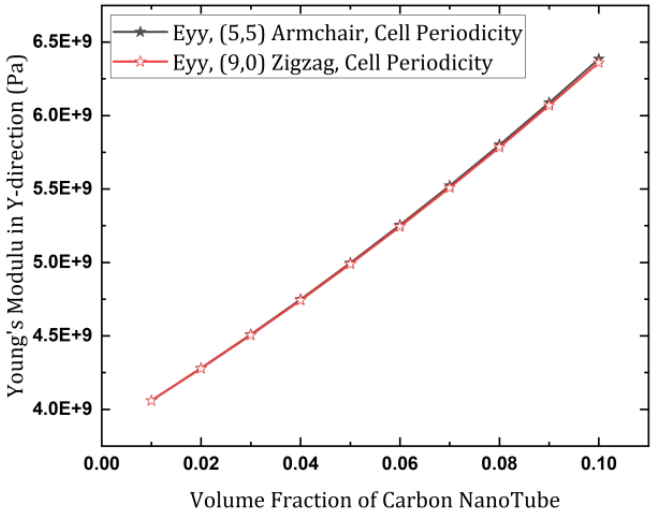

Figure 6. Young's moduli in Y-direction

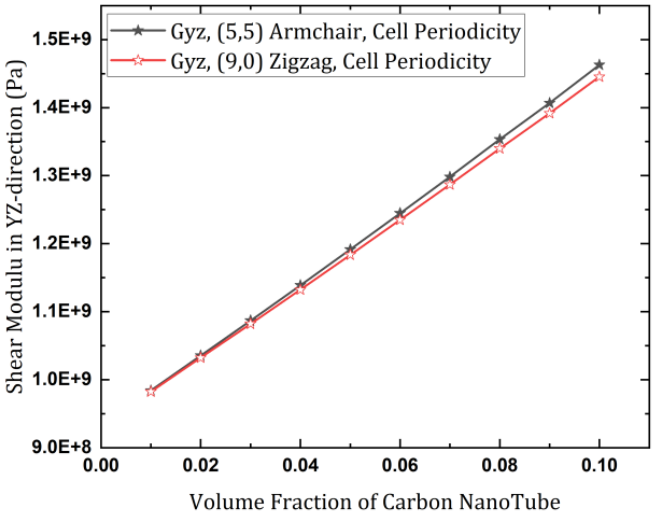

Figure 9. Shear moduli in YZ-direction

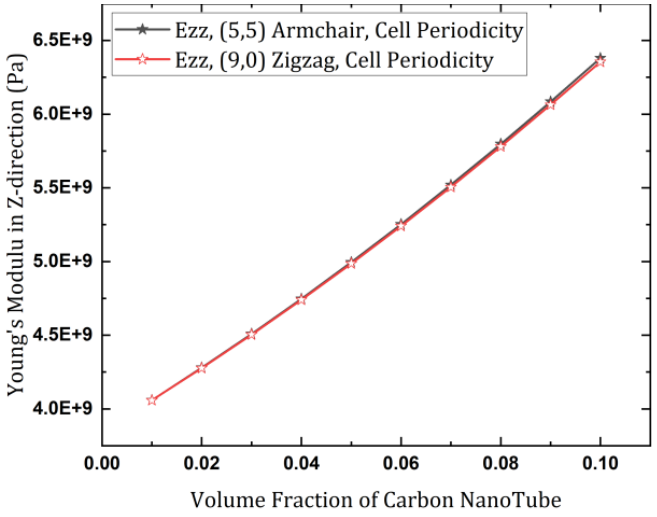

Figure 7. Young's moduli in Z-direction

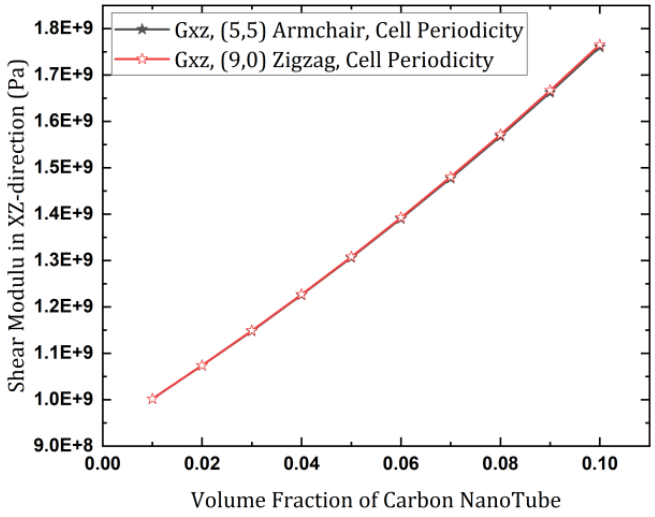

Figure 10. Shear moduli in XZ-direction

samples have varying concentrations of SWCNTs, ranging from 10% to 20%. These tables and figures illustrate the effect of the nanotube concentration on the mechanical performance of the composite materials.

It is noted that these figures collectively offer a comprehensive view of how the mechanical properties of the polymer-nanotube composites are influenced by the inclusion of (5,5) Armchair and (9,0) zigzag SWCNTs at

concentrations ranging from 11% to 20%. They are essential in understanding the relationship between SWCNT content and the enhancement of mechanical performance in these composite materials, which can have significant implications for various engineering and material science applications.

Tables 7 and 8, along with Figures 11–13, present the Young's moduli for polymer-nanotube composite materials incorporating varying concentrations of (5,5) Armchair and (9,0) Zigzag single-walled carbon nanotubes (SWCNTs). These results illustrate the changes in composite stiffness as nanotube content increases from 11% to 20%. Notably, a substantial enhancement in the Young's modulus of the reinforced PMMA is observed, indicating a marked increase in the material's stiffness with higher nanotube concentrations.

When incorporating 11% concentration of (5,5) Armchair SWCNTs into a PMMA matrix, a substantial increase in the axial Young's modulus E_{xx} is observed, reaching a value of 1.44E11 Pa. Doubling the nanotube concentration to 20% further enhances the axial Young's modulus, bringing it to 2.86258E11 Pa. A similar trend is noted for PMMA reinforced with (9,0) Zigzag SWCNTs at 11%, where the Young's modulus E_{xx} reaches 1.45656E11 Pa. Increasing the nanotube concentration to 20% results in a further increase in the axial Young's modulus, now reaching 2.72168E11 Pa (see Table 7, 8 and Figure 11).

The analysis of Young's modulus E_{yy} along the y-direction indicates that an increase in the concentration of (5,5) armchair single-walled carbon nanotubes (SWCNTs) within a PMMA nanocomposite matrix enhances its stiffness. At a concentration of 11% (5,5) armchair SWCNTs, E_{yy} is measured at 2.59923E9 Pa. Increasing the concentration to 20% results in a significant increase in E_{yy} to 1.00E10 Pa. In comparison, PMMA reinforced with 11% (9,0) zigzag SWCNTs yields a Young's modulus of 2.45526E9 Pa, which rises to 9.914E9 Pa at a 20% concentration (refer to Tables 7, 8 and Figure 12).

Tables 9–10 and Figures 14–16 below provide a comparative analysis of the shear moduli of PMMA reinforced with two different types of carbon nanotubes: (5,5) Armchair and (9,0) Zigzag SWCNTs.

The shear moduli of the nanocomposite materials exhibit significant variations as the concentration of SWCNTs changes. Specifically, at a 11% concentration of (5,5) Armchair SWCNTs, the shear modulus, G_{xy}, of the nanocomposite is measured at 1.75422E9 Pa, representing a notable increases. Increasing the concentration to 20% raises the shear modulus to 2.98686E9 Pa. A similar trend is observed when introducing 11% of (9,0) Zigzag SWCNTs into PMMA matrix, resulting in a shear modulus, G_{xy}, of 1.76054E9 Pa. With a subsequent increase to 20% concentration, the shear modulus increases to 2.99318E9 Pa (refer to Tables 9–10 and Figure 14).

Table 7. Young's Moduli of nanocomposite PMMA-(5,5) Armchair, Cell Periodicity

VF (%)	E_{xx} (Pa)	E_{yy} (Pa)	E_{zz} (Pa)
0.11	1.44000E11	2.59923E9	6.39162E9
0.12	1.61323E11	3.217E9	6.69813E9
0.13	1.74773E11	3.81382E9	7.02238E9
0.14	1.88886E11	4.52058E9	7.32003E9
0.15	2.03000E11	5.24567E9	7.68861E9
0.16	2.16734E11	5.9341E9	8.0306E9
0.17	2.30516E11	6.71416E9	8.38144E9
0.18	2.44629E11	7.45757E9	8.75002E9
0.19	2.58742E11	8.3083E9	9.1452E9
0.20	2.86258E11	1.000E10	9.96976E9

Table 8. Young's Moduli of nanocomposite PMMA-(9,0) Armchair, Cell Periodicity

VF (%)	E_{xx} (Pa)	E_{yy} (Pa)	E_{zz} (Pa)
0.11	1.45656E11	2.45526E9	6.32069E9
0.12	1.59868E11	3.08873E9	6.63607E9
0.13	1.73503E11	3.72482E9	6.94385E9
0.14	1.87667E11	4.35829E9	7.26810E9
0.15	2.01926E11	5.1017E9	7.61009E9
0.16	2.15898E11	5.82678E9	7.95207E9
0.17	2.29870E11	6.55187E9	8.32065E9
0.18	2.43985E11	7.34763E9	8.68036E9
0.19	2.58197E11	8.12768E9	9.06541E9
0.20	2.72168E11	9.914E9	9.89623E9

Table 9. Shear Moduli of nanocomposite PMMA-(5,5) Armchair, Cell Periodicity

VF (%)	G_{xy} (Pa)	G_{xz} (Pa)	G_{yz} (Pa)
0.11	1.75422E9	1.75422E9	1.45936E9
0.12	1.85769E9	1.85453E9	1.51930E9
0.13	1.96071E9	1.95755E9	1.57611E9
0.14	2.07638E9	2.07006E9	1.63774E9
0.15	2.19251E9	2.18302E9	1.69936E9
0.16	2.30818E9	2.29869E9	1.76436E9
0.17	2.43334E9	2.43018E9	1.82598E9
0.18	2.56167E9	2.55218E9	1.89772E9
0.19	2.70219E9	2.68954E9	2.03445E9
0.20	2.98686E9	2.98053E9	2.1128E9

Table 10. Shear Moduli of nanocomposite PMMA-(9,0) Armchair, Cell Periodicity

VF (%)	G_{xy} (Pa)	G_{xz} (Pa)	G_{yz} (Pa)
0.11	1.76054E9	1.86085E9	1.44107E9
0.12	1.86673E9	1.96387E9	1.49932E9
0.13	1.97336E9	2.07955E9	1.55276E9
0.14	2.08271E9	2.19251E9	1.61102E9
0.15	2.19522E9	2.31451E9	1.67433E9
0.16	2.31722E9	2.44238E9	1.73595E9
0.17	2.44238E9	2.56167E9	1.79758E9
0.18	2.57071E9	2.71168E9	1.85776E9
0.19	2.70536E9	2.85266E9	1.92612E9
0.20	2.99318E9	2.98686E9	2.06599E9

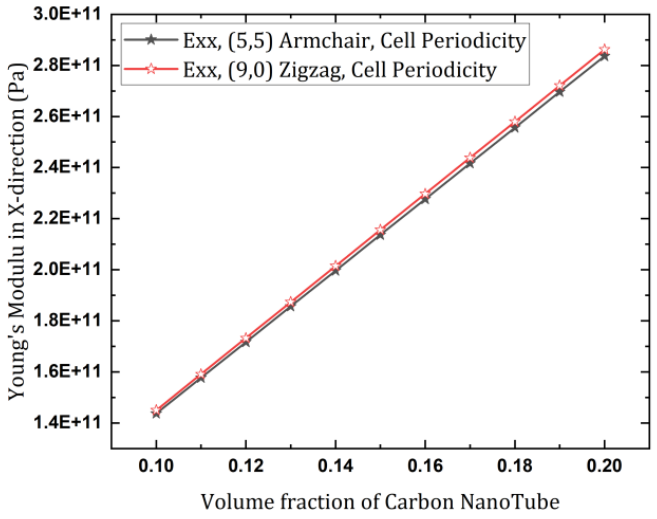

Figure 11. Young's moduli in X-direction

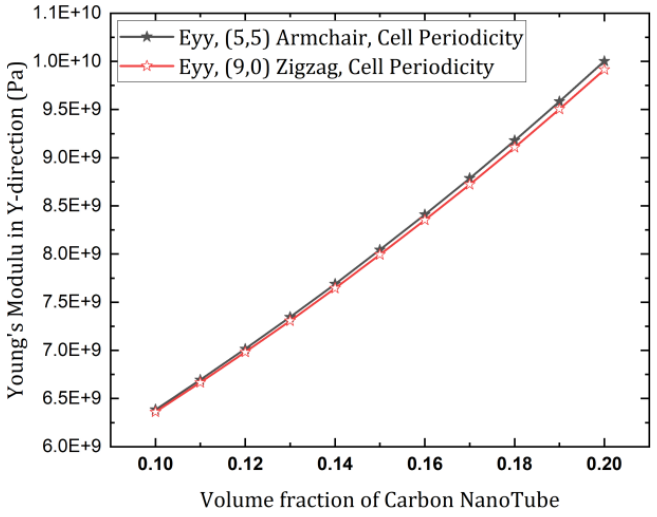

Figure 12. Young's moduli in Y-direction

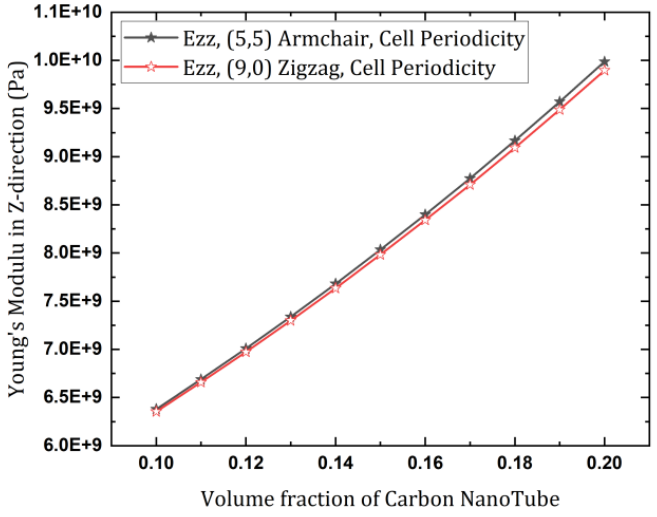

Figure 13. Young's moduli in Z-direction

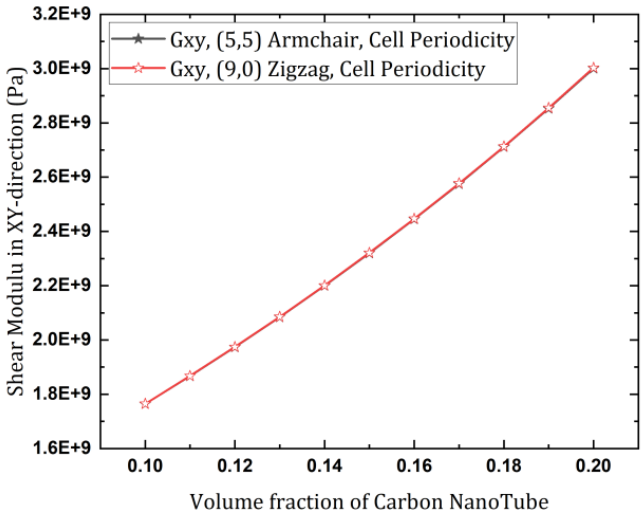

Figure 14. Shear moduli in XY-direction

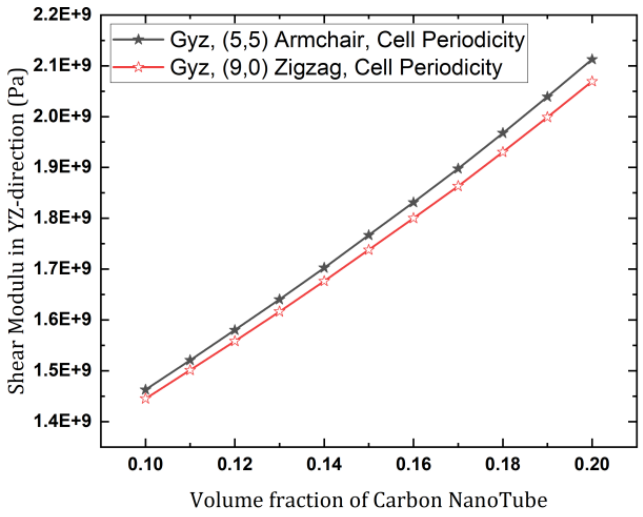

Figure 15. Shear moduli in YZ-direction

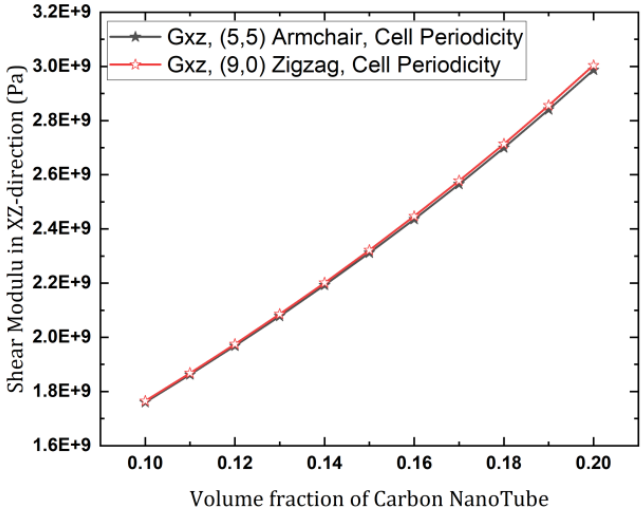

Figure 16. Shear moduli in XY-direction

This trend persists when examining the shear modulus, G_{yz}, of the nanocomposite. At a 11% concentration of (5,5) Armchair SWCNTs, this shear modulus is 1.45936E9 and increasing the concentration to 20% raises it has the value of 2.1128E9 Pa. For PMMA reinforced with 11% of (9,0) Zigzag SWCNTs, the shear modulus, G_{yz}, is 1.44107E9 Pa at a 11% concentration, and it increases to 2.06599E9 Pa at a 20% concentration of (9,0) Zigzag SWCNTs (refer to Tables 9–10 and Figure 15).

Similarly, when analyzing the shear modulus, G_{xz}, for PMMA, at a 11% concentration of (5,5) Armchair SWCNTs, it measures 1.75422E9 Pa, and this value rises to 2.98053E9 Pa with a 20% concentration. For PMMA reinforced with 11% of (9,0) Zigzag SWCNTs, the Shear modulus, G_{xz}, is 1.86085E9 Pa at a 10% concentration and increases to 2.98686E9 Pa at a 20% concentration (see Figure 16 and Tables 9–10).

4. VERIFICATION OF AXIAL YOUNG'S MODULUS

The Rules of Mixtures (ROMs) are useful for predicting the properties of the composite materials, where the constituents are macroscopic and exhibit well-defined bulk properties. However, for nanocomposites which contain nanoparticles or nanofillers dispersed within a matrix material, these rules often fall short in predicting the elastic properties accurately for several reasons: Size effects, interface effects, distribution and agglomeration, nanoparticle shape and quantum mechanical effects.

ROM typically predicts the Young's modulus in the longitudinal (or axial) direction of the composite material, not the transverse direction. Young's modulus in the longitudinal direction, E_{xx}, represents the material stiffness along the axis aligned with the predominant orientation of the reinforcing phase in the composite. The prediction of E_{xx} using ROM is based on the assumption that the overall stiffness of the composite is proportional to the volume fractions and stiffness of the individual constituents. The formula for predicting E_{xx} using ROM as:

$$E_{Composite} = v_{cnt} \times E_{xx}^{cnt} + (1 - v_{cnt}) \times E_m \quad (8)$$

Here E_{xx}^{cnt} accounts for the longitudinal Young's modulus of the carbon nanotube, v_{cnt} for the volume fractions of the reinforcing phase (e.g., SWCNTs) and E_m for the Young's modulus of the matrix phase, respectively. It is important to note that such a prediction is specifically for the stiffness in the direction aligned with the reinforcing phase. To predict the transverse Young's modulus, E_{yy}, or other properties in different directions, we would need to consider additional factors, such as the arrangement and orientation of the reinforcing phase, the interfacial properties and the microstructure of the nanocomposite. In many cases, the experimental characterization is necessary to accurately predict properties in different directions or under different loading conditions.

In the provided Figures 17–20 and Tables 11, the axial Young's modulus is graphically presented as a function of the volume fraction. These figures and tables are the result of simulations and rules of mixture (ROM) to estimate the axial Young's modulus for different volume fractions of nanoscale composite.

These graphs illustrate how the axial Young's modulus varies with changes in the volume fraction, providing valuable insights into the mechanical behavior of the nanoscale composite under an axial displacement traduced by equation (3). This data is crucial for understanding the

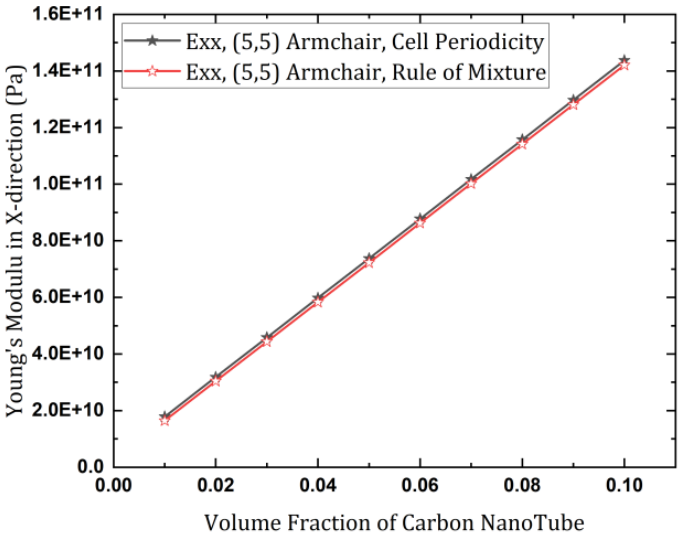

Figure 17. Axial Young's moduli in low-concentration of (5,5) armchair carbon nanotube-reinforced PMMA

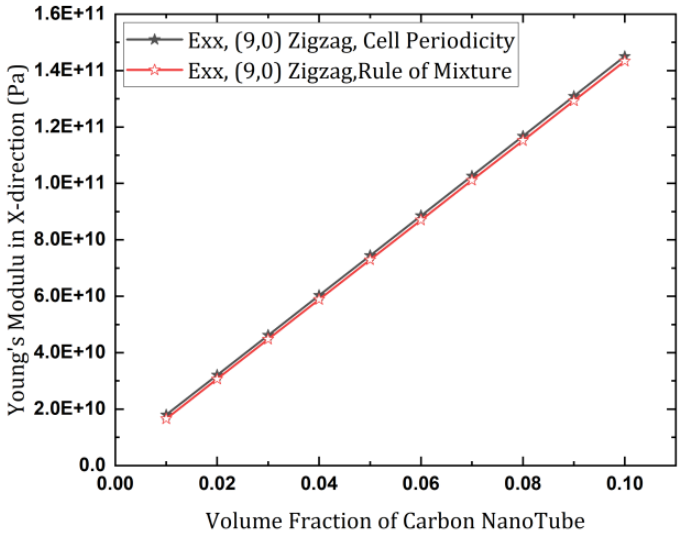

Figure 18. Axial Young's moduli in low-concentration of (9,0) zigzag carbon nanotube-reinforced PMMA

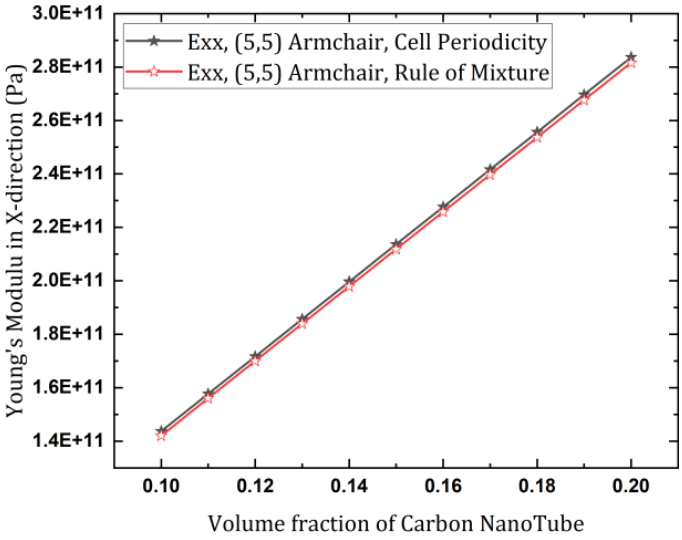

Figure 19. Axial Young's moduli in high-concentration of (5,5) armchair carbon nanotube-reinforced PMMA

Table 11. Axial Young's moduli in low-concentration cell periodicity vs rules of mixture (ROM)

VF (%)	PMMA-(5,5) armchair nanocomposite	
	Cell Periodicity	ROM
0.01	1.78320*E*10	1.54821E10
0.02	3.11143E10	2.99362E10
0.03	4.49340E10	4.38012E10
0.04	5.87537E10	5.76663E10
0.05	7.28453E10	7.16672E10
0.06	8.72994E10	8.58042E10
0.07	1.00802E11	9.9488E10
0.08	1.14894E11	1.13489E11
0.09	1.29348E11	1.27807E11
0.10	1.43439E11	1.41491E11
VF (%)	**PMMA-(9,0) zigzag nanocomposite**	
0.01	1.79619*E*10	1.6155E10
0.02	3.14314E10	3.03938E10
0.03	4.58855E10	4.48128E10
0.04	6.02943E10	5.84208E10
0.05	7.44312E10	7.23442E10
0.06	8.85228E10	8.64479E10
0.07	1.02660E11	1.00552E11
0.08	1.16479E11	1.1461E11
0.09	1.30868*E*11	1.28398E11
0.10	1.45025E11	1.42006E11
0.20	2.72168E11	2.69672E11

relationship between the volume fraction and the material prediction of Young's modulus values across a range of the stiffness, which is vital in materials science and engineering applications. The simulations and ROM enable us the volume fractions, aiding in the design and optimization of materials with specific mechanical properties. The axial Young's modulus given by *Comsol Code* and the one given by ROM equation (9) are almost the same for both nanocomposite reinforced by (5,5) Armchair SWCNTs and nanocomposite reinforced by (9,0) Zigzag SWCNTs, because in the direction of the carbon nanotube orientation which means under axial loading given by the equation (3), the interface effects, the size effect and the nanoparticle shape are less important.

Finally, the other constants stiffness cannot be checked using ROM, because the geometric effect is very large and ROM does not take into account the geometric parameters quoted previously.

5. CONCLUSION

Based on the results pointed out above, we can conclude that both PMMA reinforced with (5,5) Armchair SWCNTs compared to the pure PMMA matrix. The analysis of three-dimensional representative volume elements using COMSOL Multiphysics® Software revealed that the addition of carbon nanotubes as reinforcement significantly affects the elastic behavior of the nanocomposites. For the PMMA nanocomposite reinforced with (5,5) Armchair single wall carbon nanotubes, it was observed that the elastic modulus in all three directions (x, y, and z) increased with increasing volume fraction of the carbon nanotubes. This indicates that the presence of (5,5) Armchair single wall carbon nanotubes enhances the stiffness of the nanocomposite material. Similarly, the shear modulus in the XY, YZ, and ZX planes also exhibited an increasing trend with the addition of carbon nanotubes. In the case of PMMA nanocomposite reinforced with (9,0) Zigzag SWCNTs, the elastic modulus and shear modulus also showed an increasing trend with increasing volume fraction of the carbon nanotubes. However, the rate of increase was slightly different compared to the (5,5) Armchair SWCNTs reinforcement. The (9,0) Zigzag SWCNTs contributed to an improvement in the effective elastic properties of the nanocomposite, albeit with a different magnitude than the (5,5) Armchair single wall carbon nanotubes. These findings suggest that the choice of carbon nanotube reinforcement, whether (5,5) Armchair or (9,0) Zigzag nanotubes, can influence the resulting effective elastic properties of PMMA nanocomposites.

As we have seen above, the specific structure and symmetry of the carbon nanotubes play a crucial role in determining the extent of improvement in mechanical properties of the nanocomposite.

We emphasize that the choice of (5,5) Armchair and (9,0) Zigzag SWCNTs in our numerical simulation is not restrictive, but one can also choose other values of indices (m,n). Qualitatively, the conclusions are the same.

Finally, in this work, we have not examined nanocomposites with dispersed chiral SWCNTs. The reason for that is the fact that these nanotubes are isotropic from a mechanical point of view.

REFERENCES

[1] C. C. Okpala, "Nanocomposites – An Overview," *International Journal of Engineering Research and Development*, vol. 8, no. 11, pp. 17–23, Oct. 2013.

[2] R. Hirlekar, M. Yamagar, H. Garse, M. Vij, And V. Kadam, "Carbon Nanotubes and Its Applications: A Review," *Asian Journal of Pharmaceutical and Clinical Research*, vol. 2, no. 4, pp. 17–27, 2009.

[3] R. S. Ruoff and D. C. Lorents, "Mechanical and thermal properties of carbon nanotubes," *Carbon*, vol. 33, no. 7, pp. 925–930, 1995, doi: 10.1016/0008-6223(95)00021-5.

[4] K. Friedrich, S. Fakirov, and Z. Zhang, *Polymer Composites: From Nano- to Macro-Scale*. Boston, MA: Springer US, 2005. doi: 10.1007/b137162.

[5] Qadir, P. Pinke, and J. Dusza, "Silicon Nitride-Based Composites with the Addition of CNTs—A Review of Recent Progress, Challenges, and Future Prospects," *Materials*, vol. 13, no. 12, p. 2799, Jun. 2020, doi: 10.3390/ma13122799.

[6] L. Boumia, M. Zidour, A. Benzair, and A. Tounsi, "A Timoshenko beam model for vibration analysis of chiral single-walled carbon nanotubes," *Physica E: Low-dimensional Systems and Nanostructures*, vol. 59, pp. 186–191, May 2014, doi: 10.1016/j.physe.2014.01.020.

[7] Ribeiro, E. C. Botelho, M. L. Costa, and C. F. Bandeira, "Carbon nanotube buckypaper reinforced polymer

composites: a review," *Polímeros*, vol. 27, no. 3, pp. 247–255, Sep. 2017, doi: 10.1590/0104-1428.03916.

[8] R. K. Sahu, V. Mukherjee, T. Dash, S. K. Padhan, and B. B. Nayak, "Vibrational and electronic properties of (5,0) zigzag and (5,5) armchair carbon and SiC nanotubes using density functional theory," *Physica B: Condensed Matter*, vol. 615, p. 413074, Aug. 2021, doi: 10.1016/j.physb.2021.413074.

[9] V. Harik, "Chapter 1 - Nanotechnology of Carbon Nanotubes: Sensors, Transistors and Nano composites," in *Mechanics of Carbon Nanotubes*, V. Harik, Ed., Academic Press, 2018, pp. 1–24. doi: https://doi.org/10.1016/B978-0-12-811071-3.00001-9.

[10] H. Liu, D. Liu, F. Yao, and Q. Wu, "Fabrication and properties of transparent polymethylmethacrylate/ cellulose nanocrystals composites," *Bioresource Technology*, vol. 101, no. 14, pp. 5685–5692, Jul. 2010, doi: 10.1016/j.biortech.2010.02.045.

[11] U. Ali, K. J. Bt. A. Karim, and N. A. Buang, "A Review of the Properties and Applications of Poly (Methyl Methacrylate) (PMMA)," *Polymer Reviews*, vol. 55, no. 4, pp. 678–705, Oct. 2015, doi: 10.1080/15583724.2015.1031377.

[12] S. A. S. P. Sathurusinghe, W. M. N. A. P. B. Herath, H. A. R. Subhashini, A. M. C. S. S. Kumara, and K. R. B. Herath, "Stress concentrations near the perfectly bonded interfaces of single walled carbon nanotube reinforced composites," *International Journal of Nanotechnology and Applications*, vol. 7, no. 1, pp. 1–10, 2013.

[13] Y. Wei, N. Baskaran, H.-Y. Wang, Y.-C. Su, S. C. Nabilla, and R.-J. Chung, "Study of polymethylmethacrylate/ tricalcium silicate composite cement for orthopedic application," *Biomedical Journal*, vol. 46, no. 3, p. 100540, Jun. 2023, doi: 10.1016/j.bj.2022.05.005.

[14] K. G. de C. Monsores, A. O. da Silva, S. de S. A. Oliveira, J. G. P. Rodrigues, and R. P. Weber, "Influence of ultraviolet radiation on polymethylmethacrylate (PMMA)," *Journal of Materials Research and Technology*, vol. 8, no. 5, pp. 3713–3718, Sep. 2019, doi: 10.1016/j.jmrt.2019.06.023.

[15] A. Kausar, "Poly(methyl methacrylate) nano composite reinforced with graphene, graphene oxide, and graphite: a review," *Polymer-Plastics Technology and Materials*, vol. 58, no. 8, pp. 821–842, May 2019, doi: 10.1080/25740881.2018.1563112.

[16] Rittel and A. Brill, "Dynamic flow and failure of confined polymethylmethacrylate," *Journal of the Mechanics and Physics of Solids*, vol. 56, no. 4, pp. 1401–1416, 2008, doi: https://doi.org/10.1016/j.jmps.2007.09.003.

[17] O. Furnes *et al.*, "Prospective studies of hip and knee prostheses–The Norwegian Arthroplasty Register 1987–2004," *Scientific Exhibition AAOS, Washington DC*, 2005.

[18] A. Bistolfi, R. Ferracini, C. Albanese, E. Vernè, and M. Miola, "PMMA-Based Bone Cements and the Problem of Joint Arthroplasty Infections: Status and New Perspectives," *Materials*, vol. 12, no. 23, p. 4002, Dec. 2019, doi: 10.3390/ma12234002.

[19] R. Vaishya, M. Chauhan, and A. Vaish, "Bone cement," *Journal of Clinical Orthopaedics and Trauma*, vol. 4, no. 4, pp. 157–163, Dec. 2013, doi: 10.1016/j.jcot.2013.11.005.

[20] F. Ghasemi, A. Jahani, A. Moradi, M. H. Ebrahimzadeh, and N. Jirofti, "Different Modification Methods of Poly Methyl Methacrylate (PMMA) Bone Cement for Orthopedic Surgery Applications.," *The archives of bone and joint surgery*, vol. 11, no. 8, pp. 485–492, 2023, doi: 10.22038/ABJS.2023.71289.3330.

[21] A. Oryan, S. Alidadi, A. Bigham-Sadegh, and A. Moshiri, "Healing potentials of polymethylmethacrylate bone cement combined with platelet gel in the critical-sized radial bone defect of rats," *PLOS ONE*, vol. 13, no. 4, p. e0194751, Apr. 2018, doi: 10.1371/journal.pone.0194751.

[22] J. R. Cho and H. J. Kim, "Numerical Optimization of CNT Distribution in Functionally Graded CNT-Reinforced Composite Beams," *Polymers*, vol. 14, no. 20, p. 4418, Oct. 2022, doi: 10.3390/polym14204418.

[23] N. Anzar, R. Hasan, M. Tyagi, N. Yadav, and J. Narang, "Carbon nanotube - A review on Synthesis, Properties and plethora of applications in the field of biomedical science," *Sensors International*, vol. 1, p. 100003, 2020, doi: 10.1016/j.sintl.2020.100003.

[24] B. v. Basheer, J. J. George, S. Siengchin, and J. Parameswaranpillai, "Polymer grafted carbon nanotubes—Synthesis, properties, and applications: A review," *Nano-Structures & Nano-Objects*, vol. 22, p. 100429, Apr. 2020, doi: 10.1016/j.nanoso.2020.100429.

[25] N. Mohd Nurazzi *et al.*, "Fabrication, Functionalization, and Application of Carbon Nanotube-Reinforced Polymer Composite: An Overview," *Polymers*, vol. 13, no. 7, p. 1047, Mar. 2021, doi: 10.3390/polym13071047.

[26] A. M. Díez-Pascual, "Chemical Functionalization of Carbon Nanotubes with Polymers: A Brief Overview," *Macromol*, vol. 1, no. 2, pp. 64–83, Mar. 2021, doi: 10.3390/macromol1020006.

[27] K. Li, G. Xu, X. Huang, Z. Xie, and F. Gong, "Manufacturing of Micro-Lens Array Using Contactless Micro-Embossing with an EDM-Mold," *Applied Sciences*, vol. 9, no. 1, p. 85, Dec. 2018, doi: 10.3390/app9010085.

[28] Y. J. Liu and X. L. Chen, "Evaluations of the effective material properties of carbon nanotube-based composites using a nanoscale representative volume element," *Mechanics of Materials*, vol. 35, no. 1–2, pp. 69–81, Jan. 2003, doi: 10.1016/S0167-6636(02)00200-4.

[29] A. Allahdadian and M. Mashayekhi, "Experimental and numerical study of tensile behavior of carbon nanotube reinforced glass-epoxy composite: The multiscale approach," *Composite Structures*, vol. 304, p. 116394, Jan. 2023, doi: 10.1016/j.compstruct.2022.116394.